

Effect of Y on the Microstructure and Mechanical Properties of Mg-2Zn-1Mn Alloy

Chen Rong¹, Xu Junyao¹, Zhang Dingfei¹, Yu Daliang², Feng Jingkai¹

¹ National Engineering Research Center for Magnesium Alloys, Chongqing University, Chongqing 400044, China; ² Chongqing University of Science and Technology, Chongqing 401331, China

Abstract: The microstructure and mechanical response of as-cast and extruded Mg-2Zn-1Mn-XY alloys ($X=0, 0.8, 2.2$, wt%) were investigated by optical microscope (OM), scanning electron microscope (SEM) with X-ray energy dispersive spectrometer (EDS), and X-ray diffractometer (XRD). The results reveal that the addition of Y not only decreases the grain sizes of both as-cast and extruded alloys, but also effectively reduces the basal texture intensity of extruded alloys, which are the two key reasons for the improvement of the strength and ductility of Mg-2Zn-1Mn-XY alloys, simultaneously. The optimized Mg-2Zn-1Mn-XY alloy after extrusion exhibits an attractive mechanical performance. Compared with those of the matrix material Mg-2Zn-1Mn, its yield strength increases from 164 MPa to 204 MPa, the ultimate tensile strength increases from 237 MPa to 298 MPa, and the elongation increases from 12% to 18%.

Key words: Mg-Zn-Mn alloy; yttrium; microstructure; mechanical properties; texture

Recently, Mg-Zn-Mn alloy has received wild concern because of its excellent performance and relatively low cost [1-3]. It is a new kind of high performance wrought magnesium alloy with pronounced response to age-hardening, which has great potential for improving the strength by various heat treatments and micro-alloying. Zhang et al [4,5] developed the Mg-6Zn-1Mn alloy treated by two-step aging, which exhibits high strength including 310 MPa of yield strength, 340 MPa of ultimate tensile strength, but a relatively poor elongation of 6.5%. For this alloy, the high zinc content increases the strength of the alloy while sacrificing the plasticity of the material. In order to enhance the ductility of Mg-Zn-Mn alloy, ZM21 with relatively lower zinc content was investigated by Lv et al [6], and it was found that 13.7% elongation can be achieved when this alloy is extruded at 420 °C. But, it is not surprising that the strength of ZM21 is just 0.2% proof strength of about 171 MPa, and ultimate tensile strength is 251 MPa. Therefore, we can think that it is difficult to meet the requirements of ensuring the strength and toughness of the al-

loy only by changing the content of zinc.

Alloying design is an effective way for improving mechanical properties of metallic materials, including magnesium alloys [7]. In the last decade, the effect of rare earth (RE) alloying elements (such as Y, Gd, Ce and Nd) has gained more and more attention as it can refine the crystalline structure, enhance the mechanical properties and improve the processing performance [8-11]. Among them, yttrium (Y) has received particular attention, because it is one of the most abundant elements among the rare earth element. Chen et al [12] have found that the addition of Y improves the mechanical properties of Mg-5Sn-3Zn alloy effectively, especially the elongation, and Mg-5Sn-3Zn-0.5Y has the best comprehensive mechanical properties, whose elongation reaches 19.1%, 5.1% higher than 14.1% of Mg-5Sn-3Zn alloy. Some researchers have discovered that the Mg-Zn-Y alloy series are rich in ternary intermetallic compounds, including icosahedral quasicrystalline *I*-phase (Mg_3Zn_6Y), face centered cubic *W*-phase ($Mg_3Zn_3Y_2$), and long period stacking ordered (LPSO) *X*-phase ($Mg_{12}ZnY$),

Received date: July 07, 2018

Foundation item: National Key Research and Development Program of China (2016YFB0301101); National Key Basic Research Program of China (2013CB632200); Fundamental Research Funds for the Central Universities (106112017CDJPT130003); National Natural Science Foundation of China (51201190, 51571040, 51531002)

Corresponding author: Xu Junyao, Ph. D., Associate Professor, College of Materials Science and Engineering, Chongqing University, Chongqing 400044, P. R. China, Tel: 0086-23-65102466, E-mail: junyaoxu@cqu.edu.cn

Copyright © 2019, Northwest Institute for Nonferrous Metal Research. Published by Science Press. All rights reserved.

which influence the mechanical performance of alloys [13-15]. Singh et al [16] have observed that the strength of Mg-Zn-Y alloy increases with increasing the quantity of *I*-phase. However, it was reported that the presence of *W*-phase will degrade the mechanical properties of the alloys [17]. The *X*-phase was also recognized to be a superb strengthening phase due to its unique crystal structure, high strength and deformation difficulty at room temperature [18].

Except the effect of refining grain size, numerous investigations have been done to prove that the addition of Y can also produce more random orientations during hot extruding [19, 20]. It is well known that the poor formability of magnesium alloys at room temperature is due to their strong basal texture and a lack of adequate deformation systems [21]. In fact, the unfavorable mechanical response of Mg alloys with hexagonal close packed (hcp) structure can be attributed mostly to their tendency of forming very sharp textures [22-24]. Therefore, the ability to randomize the texture of wrought magnesium alloys has some positive influences, such as reducing the tension-compression strength asymmetry as well as the potential for improving the secondary formability.

In the present study, the effect of Y content varying from 0 to 2.2 wt% on the microstructure, mechanical properties and texture of Mg-Zn-Mn-XY alloys was studied by optical microscope, scanning electron microscope with X-ray energy dispersive spectrometer, X-ray diffractometer, and the room temperature tensile test.

1 Experiment

The chemical composition of the materials used in this work was analyzed by the X-ray fluorescence spectrometer (Shimadzu XRF1800), and the results are presented in Table 1. The as-cast ingots were homogenized at 500 °C for 12 h and then cooled in air. After homogenization, the ingots were hot-extruded into rods with a diameter of 16 mm. The extrusion ratio was 25:1 and the extrusion temperature was 450 °C.

All the as-cast and extruded alloy samples for metallography observation were ground with 1200 grit SiC paper. As-cast alloys were etched by 1 mL nitric acid and 20 mL ethyl alcohol. Extruded alloys were etched by 5 g picric acid, 1 mL acetic acid and 8 mL ethyl alcohol. The microstructures of these alloys were observed by optical microscope (OM, Olympus Measuring Laser, Microscope OLS4000) and scanning electron micro-

scope (SEM, Tescan VEGA 3) equipped with X-ray energy dispersive spectrometer (EDS). Phase analysis was determined by X-ray diffractometer (XRD) using Cu K α radiation with a scanning angle of 10°~90° and a scanning rate of 4°/min. The crystallographic texture of the extruded alloys was determined by XRD using Cu K α radiation (wavelength $\lambda=0.154\ 06\ \text{nm}$) at 45 kV and 40 mA and the sample tilt angle ψ ranged from 0° to 70°.

The extruded samples were machined into cylindrical tensile specimens with a gauge size of 5 mm in diameter and 35 mm in length. The room temperature tensile tests were performed using CMT-5105 universal material testing machine at a strain rate of 3.0 mm/min. Yield strength (YS) was determined as 0.2% proof stress, and ultimate tensile strength (UTS) and fracture elongation were obtained based on the average of three tests. Fracture surface was investigated by SEM.

2 Results

2.1 Microstructure of as-cast alloys

The optical microstructures and BSE images of as-cast ZM21, ZM21-0.8Y, and ZM21-2.2Y alloys are shown in Fig.1 and Fig.2, respectively. The as-cast alloy consists of α -Mg matrix and a compound phase continuously distributed on the grain boundary. The α -Mg is dendritic, and with the increase of Y element content, the precipitates on the grain boundary increase and the dendritic structure is refined. The eutectic compounds are dispersed almost along grain boundaries, only few inside the grains. According to the EDS results presented in Table 2, both the particles and laminar structures are composed of Mg, Zn and Y. From the microstructure, it can be seen that with the increase of the Y content, more second phase precipitates along the grain boundaries.

Fig.3 shows the X-ray diffraction patterns of as-cast alloys containing different amounts of Y. As indicated in the patterns, when the content of Y is 0.8 wt%, the Zn/Y weight ratio is close to 2.65, and the phases are α -Mg, *I*-phase and *W*-phase. As the content of Y increases to 2.2 wt%, the Zn/Y weight ratio is 0.84, and the phases change to α -Mg, *W*-phase and *X*-phase. When the content of Y is higher than the content of Zn, the LPSO structure *X*-phase can be formed. This result is coincident well with Ref.[25-27].

2.2 Microstructure of as-extruded alloys

Fig.4 shows the BSE micrographs of as-extruded ZM21-XY ($X=0, 0.8, 2.2$) alloys parallel to the extrusion direction. It is obvious that the grains are greatly refined with the addition of Y element after extrusion deformation. The EDS results (listed in Table 3) show that the composition of the second phase of the as-extruded alloys is the same as that of the as-casted alloys. Dynamic recrystallization occurs during the hot extrusion. The grains are averagely refined with the increase of the amount of Y element. The white bright spots in Fig.4a are the Mn element which should be mostly dissolved into the as-cast matrix. Then after the hot extrusion treatment, a small amount

Table 1 Chemical composition of Mg-2Zn-1Mn-XY alloys (wt%)

Alloy	Zn	Mn	Y	Mg
Mg-2Zn-1Mn (ZM21)	1.98	0.71	0	Bal.
Mg-2Zn-1Mn-0.8Y (ZM21-0.8Y)	2.12	0.81	0.80	Bal.
Mg-2Zn-1Mn-2.2Y (ZM21-2.2Y)	1.85	0.75	2.19	Bal.



Fig.1 Optical microstructures of the as-cast magnesium alloys: (a) ZM21, (b) ZM21-0.8Y, and (c) ZM21-2.2Y

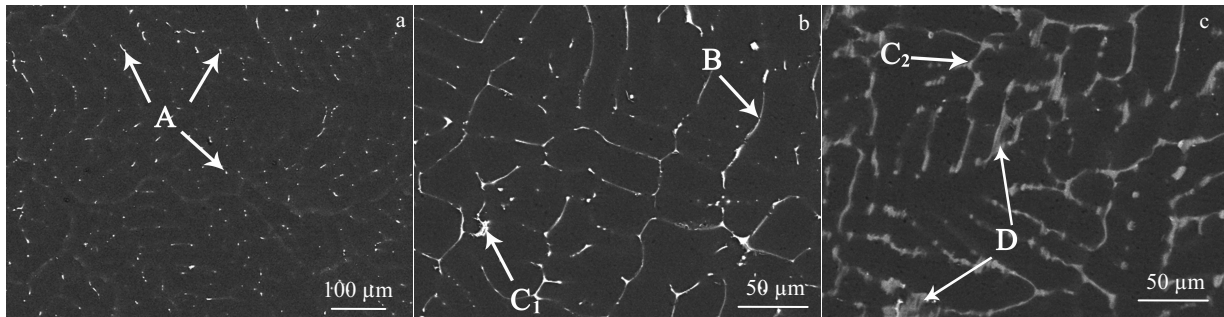


Fig.2 BSE images of the as-cast magnesium alloys: (a) ZM21, (b) ZM21-0.8Y, (c) ZM21-2.2Y

Table 2 EDS results of point A, B, C and D in Fig.2

Point	Composition/at%			Phase
	Mg	Zn	Y	
A	96.56	3.44	-	Mg ₇ Zn ₃
B	85.70	11.32	2.98	Mg ₃ Zn ₆ Y
C ₁	86.50	7.92	5.58	Mg ₃ Zn ₃ Y ₂
C ₂	89.34	6.49	4.17	
D	90.94	4.45	4.61	Mg ₁₂ ZnY

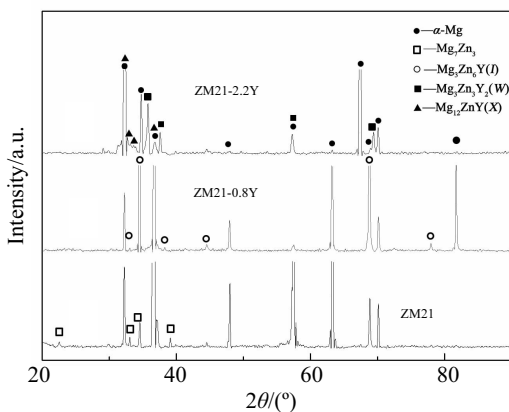


Fig.3 XRD patterns of as-cast magnesium alloys

of fine Mn particles precipitate in the structure, studied by Qi et al [28]. Comparing Fig.2 and Fig.4, especially 2b and 4b, 2c and 4c, it can be found that the secondary phases are distributed mostly along the grain boundary in the as-cast alloys. After hot extrusion, the secondary phases are broken into pieces. As can be seen from Fig.4c, the number of the second phases obviously increases with the increase of Y content, and the fragmented second phase particle bands are distributed along the extrusion direction in the as-extruded ZM21-2.2Y alloy.

2.3 Texture of as-extruded alloys

Fig.5a~5c show the (0002) and (10 $\bar{1}$ 0) pole figures of extruded ZM21-XY alloys perpendicular to the extrusion direction. It is well known that magnesium alloys have apparently preferred grain orientation and basal plane (0002) is parallel to the extruded direction (ED) during hot extrusion. The texture of ZM21 is a normal extruded fiber texture with an intensity of 4.993, as shown in Fig.5a. When the addition of Y is 0.8 wt%, it does not change the texture type but the basal texture intensity decreases slightly to 4.615. Furthermore, the texture intensity drops to 2.764 when the Y element content increases to 2.2 wt%. It can be seen that Y can efficiently weaken the basal texture, and cause a low basal texture intensity. Kula et al [29] reported that Y strengthens most <c+a> slip system,

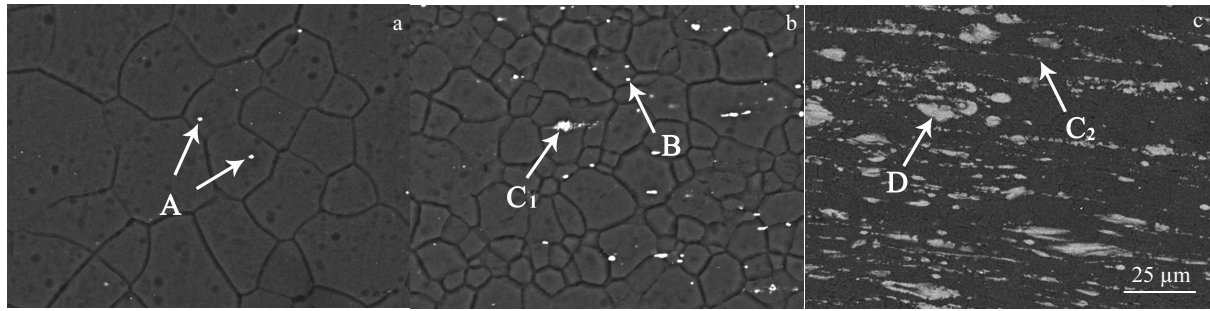


Fig.4 BSE images of the as-extruded magnesium alloys: (a) ZM21, (b) ZM21-0.8Y, and (c) ZM21-2.2Y

Table 3 EDS results of point A, B, C and D in Fig.4

Point	Composition/at%				Phase
	Mg	Zn	Mn	Y	
A	32.64	-	67.36	-	Mn
B	77.53	19.32	-	3.15	Mg ₃ Zn ₆ Y
C ₁	67.93	18.48	-	13.59	Mg ₃ Zn ₃ Y ₂
C ₂	70.18	16.74	-	13.08	Mg ₃ Zn ₃ Y ₂
D	91.57	4.47	-	3.95	Mg ₁₂ ZnY

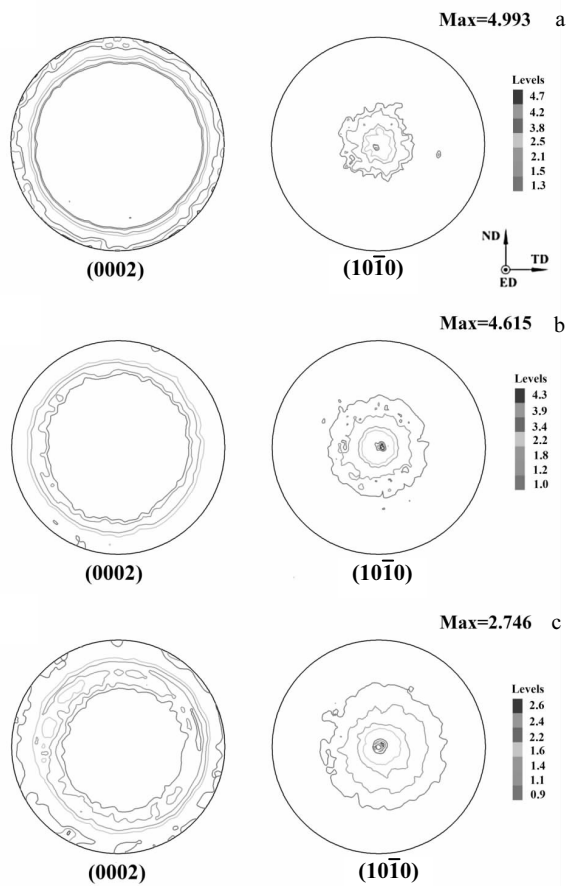


Fig.5 Basal (0002) and (10 $\bar{1}0$) pole figures of as-extruded magnesium alloys: (a) ZM21, (b) ZM21-0.8Y, and (c) ZM21-2.2Y

which exhibits a monotonic increase in CRSS with the Y addition at different rates.

2.4 Mechanical properties of as-extruded alloys

The room temperature mechanical properties of as-extruded ZM21-XY alloys are shown in Fig.6. It indicates that with the increase of Y content, the yield strength, ultimate tensile strength and elongation can be improved simultaneously, and the tensile properties are remarkable. The YS, UTS and elongation rate (δ) of the ZM21-2.2Y alloy rise to 204 MPa, 298 MPa and 18%, which are 40 MPa, 61 MPa and 6% higher than those of ZM21, respectively.

Fig.7a~7f show the SE and BSE images of the tensile fracture surface of ZM21 alloys with different contents of Y tested at room temperature. From Fig.7a and 7d, it can be clearly seen that in the original ZM21 alloy, the tensile fracture surface has typical features of brittle fracture, including mixed fracture, cleavage plane and tearing ridge. When Y content is 0.8 wt%, except for the tearing ridge and cleavage plane, dimples are also observed in the fracture surface. This means that the material undergoes a brittle and ductile mixed fracture. When Y content increases to 2.2 wt%, only a large number of small and uniform dimples are observed on the fracture surface, and some of the dimples have a second phase particle

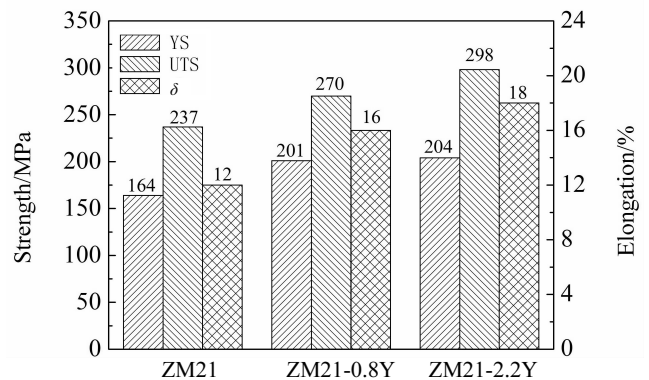


Fig.6 Mechanical properties of as-extruded ZM21-XY alloys

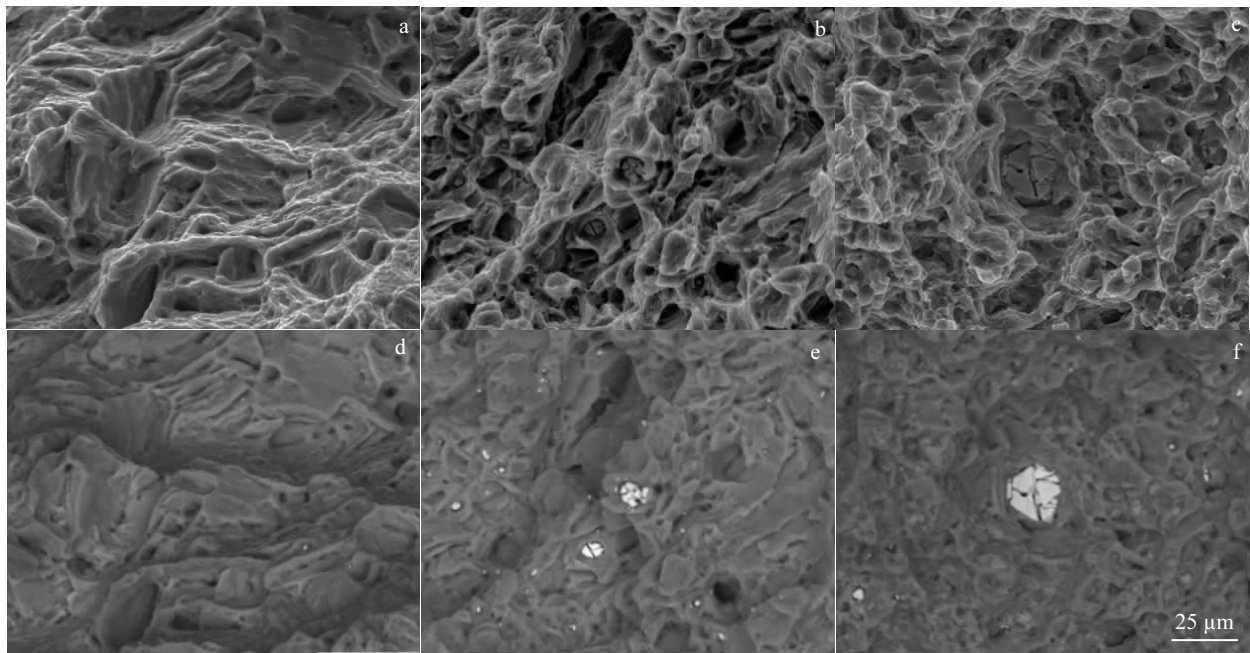


Fig.7 SE and BSE fracture images of as-extruded ZM21-XY alloys: (a, d) ZM21, (b, e) ZM21-0.8Y, and (c, f) ZM21-2.2Y

at the bottom of many voids, indicating that the fracture of the alloy changes from brittle to ductile rupture with increasing the Y content.

3 Discussion

The tensile results show that Y element can influence the mechanical properties of extruded Mg-Zn-Mn alloys. According to the previous research, the phase components of the as-cast and as-extruded Mg-Zn-Mn-Y alloys mainly consist of α -Mg, *I*-phase, *W*-phase and *X*-phase, depending on the Zn/Y weight ratio^[30]. The second phase content is critical to the mechanical properties of the extruded alloy. *I*-phase is considered to be a special strengthening phase in a ductile material because of its high hardness and low interfacial energy^[31]. Furthermore, the LPSO *X*-phase possesses lots of exceptional characteristics, such as high strength and hardness due to its unique crystal structure. And as reported, there is a stable coherent interface between the *X*-phase and the α -Mg matrix, which is important for the strength of the alloy^[32, 33]. What's more, on account of weaker atomic bonding to the Mg matrix, the existence of cubic *W*-phase reduces the mechanical performances^[34].

From the microstructure of ZM21-XY alloy, it can be concluded that Y can significantly refine the grain size and narrow the grain boundary. In the solidification process of casting, Y concentrates in the front of the solid-liquid interface because of the limitation of diffusion kinetics, so the trend of the constitutional supercooling of the solid-liquid interface increases, and thus the branching process is intensified^[35-37]. At

the same time, the intermetallic compounds with high melting points containing Y element are dispersed at grain boundaries, which results in the extension of the supercooled region in front of the solid-liquid interface, thereby inhibiting the grain growth^[38, 39]. Therefore, the second dendrites increase. Meanwhile, the dendrite spacing decreases and eventually refines the grain.

Since the extrusion temperature (450 °C) is higher than the recrystallization temperature, the dynamic recrystallization occurs during hot extrusion. And the recrystallized grains are refined, equiaxed and homogeneous. In general, hot extrusion can make the second phases precipitate along the grain boundary or inside the grains. These dispersed second phase particles can effectively retard the growth of the recrystallized grains to achieve the effect of refining grains. As shown in Fig.4, in all of the extruded alloys, the recrystallization takes place and the grain sizes are obviously refined because of the addition of Y. According to the Hall-Petch equation, the decrease of the grain size will result in the increase in yield strength of the material^[1, 40]. From Fig.6, it can be seen that the results of tensile test of ZM21-XY are in accordance with Hall-Petch relationship. The addition of a small amount of Y element significantly increases the yield strength from 164 MPa to 204 MPa.

It is worth noting that when Y content increases from 0.8 wt% to 2.2 wt%, there is little change in the yield strength. However, the ultimate tensile strength increases by about 30 MPa. This should be attributed to more precipitation of second phase particles and the reduction of texture intensity in

ZM21-2.2Y. According the precipitate hardening theory, the precipitates affect both the yield strength and the ultimate strength. Guo et al^[41] reported that texture plays an important role in the strength of Mg alloy. However, they reported that texture greatly affects the yield strength, while does not pose a great effect on the ultimate strength. Therefore, we considered that the higher ultimate strength of the alloy with a higher content of Y is mainly ascribed to the higher density of precipitate. The alloy with a lower content of Y causes a lower density of precipitates, but a stronger texture. This finally results in a similar yield strength but different ultimate strengths of the two alloys.

In general, these second particles increase the work-hardening effect, as well as decrease the elongation of materials. However, in our study, the elongation of ZM21-2.2Y alloy is 18%, which is 2% larger than 16% of ZM21-0.8Y. Kim et al^[42] indicated that the macroscopic mechanical behavior and deformation behavior of polycrystalline magnesium alloys not only obey the Hall-Petch relationship, but also are affected by crystallographic textures. Agnew et al^[43] pointed out that the addition of yttrium (Y) in magnesium can increase the activity of the nonbasal $\langle c+a \rangle$ slip mode, which can help explain their improved ductility since c -axis compression can be accommodated, and efficiently increase the plastic deformation of magnesium alloys. Bohlen et al^[44] showed that recrystallized grains in a hot extruded bar containing Y have orientations quite different from the $\langle 10\bar{1}0 \rangle$ fiber texture of deformed grains. It is generally recognized that the addition of rare earth elements results in significant texture changes during the extrusion of Mg alloys, including a randomization of the texture, i.e. significantly weaker textures and the appearance of a new texture component after processing, sometimes named as the “rare earth component”^[45, 46]. In our case, the (0002) basal fiber texture of ZM21-2.2Y is much less than that of ZM21-0.8Y, weakened from 4.615 to 2.746, which should be the major reason for the increase in elongation of alloys with Y element addition.

4 Conclusions

1) With the addition of Y, the grains of ZM21-XY ($X=0, 0.8, 2.2$) alloys in as-cast and as-extruded state are refined, and plenty of ternary intermetallic compounds of Mg-Zn-Y phases are formed at the grain boundaries.

2) Y addition in as-extruded ZM21 alloy can effectively weaken the basal texture, whose intensity decreases from 4.993 to 2.764.

3) The mechanical properties of ZM21-XY increase with the addition of Y. Among the studied alloys, ZM21-2.2 exhibits a supreme mechanical performance with the yield strength of 204 MPa, ultimate tensile strength of 298 MPa and an elongation of 18%, improved by about 40 MPa, 61 MPa and 6% compared with those of the as-extruded ZM21 alloy (164 MPa, 237 MPa and 12%), respectively.

References

- Hu G S, Zhang D F, Guo F et al. *Journal of Rare Earths*[J], 2014, 32(1): 52
- Huang D D, Liu S H, Xu H H et al. *Journal of Alloys and Compounds*[J], 2016, 688: 1115
- Liu X W, Sun J K, Zhou F Y et al. *Materials & Design*[J], 2016, 94: 95
- Zhang D F, Shi G L, Dai Q W et al. *Transactions of Nonferrous Metals Society of China*[J], 2008, 18(S1): 59
- Zhang D F, Shi G L, Zhao X B et al. *Transactions of Nonferrous Metals Society of China*[J], 2011, 21(1): 15
- Lv B J, Peng J, Peng Y et al. *Journal of Magnesium and Alloys*[J], 2013, 1(1): 94
- Hu G S, Xing B, Huang F L et al. *Journal of Alloys and Compounds*[J], 2016, 689: 326
- Liu X, Zhang Z Q, Le Q C et al. *Journal of Magnesium and Alloys*[J], 2016, 4(3): 214
- Huang S, Wang J F, Hou F et al. *Materials Science and Engineering A*[J], 2014, 612: 363
- Gao L, Luo A A. *Materials Science and Engineering A*[J], 2013, 560: 492
- Wang S D, Xu D K, Wang B J et al. *Materials & Design*[J], 2015, 84: 185
- Chen Y A, Wang Y, Gao J J. *Journal of Alloys and Compounds*[J], 2018, 740: 727
- Xu D K, Liu L, Xu Y B et al. *Journal of Alloys and Compounds*[J], 2006, 426(1-2): 155
- Tahreem N, Zhang D F, Pan F S et al. *Materials & Design*[J], 2015, 87: 245
- Tahreem N, Zhang D F, Pan F S et al. *Journal of Alloys and Compounds*[J], 2014, 615: 424
- Singh A, Watanabe M, Kato A et al. *Materials Science and Engineering A*[J], 2004, 385(1): 382
- Xu D K, Liu L, Xu Y B et al. *Materials Science and Engineering A*[J], 2007, 443(1-2): 248
- Yamasaki M, Hagihara K, Inoue S et al. *Acta Materialia*[J], 2013, 61(6): 2065
- Hantzsche K, Bohlen J, Wendt J et al. *Scripta Materialia*[J], 2010, 63(7): 725
- Sandlöbes S, Zaeferrer S, Schestakow I et al. *Acta Materialia*[J], 2011, 59(2): 429
- Wang J, Zhang X, Lu X et al. *Journal of Magnesium and Alloys*[J]. 2016, 4(3): 207
- Al-Samman T, Molodov K D, Molodov D A et al. *Acta Materialia*[J], 2012, 60(2): 537
- Hantzsche K, Bohlen J, Wendt J et al. *Scripta Materialia*[J], 2010, 63(7): 725
- Sanjari M, Kabir A S H, Farzadfar A et al. *Journal of Materials Science*[J], 2014, 49(3): 1426
- Yan B S, Dong X P, Ma R et al. *Materials Science and Engineering A*[J], 2014, 594: 168
- Yang K, Zhang J, Zong X et al. *Materials Science and Engineering A*[J], 2014, 594: 168

- neering A[J], 2016, 669: 340
- 27 Yamasaki M, Hashimoto K, Hagihara K et al. *Acta Materialia*[J], 2011, 59(9): 3646
- 28 Qi F G, Zhang D F, Zhang X H et al. *Materials Science and Engineering A*[J], 2014, 593: 70
- 29 Kula A, Jia X, Mishra R K et al. *International Journal of Plasticity*[J], 2017, 92: 96
- 30 Lee J Y, Kim D H, Lim H K et al. *Materials Letters*[J], 2005, 59(29-30): 3801
- 31 Wan D Q, Li J J, Yu T. *Rare Metal Materials and Engineering*[J], 2015, 44(11): 2651
- 32 Shao X H, Yang Z Q, Ma X L. *Acta Materialia*[J], 2010, 58(14): 4760
- 33 Li C Q, Xu D K, Zeng Z R et al. *Materials & Design*[J], 2017, 121: 430
- 34 Li Zhumin, Wan Diqing, Yi H et al. *Journal of Magnesium and Alloys*[J], 2017, 5(2): 217
- 35 Liu L Z, Chen X H, Pan F S et al. *Materials Science and Engineering A*[J], 2015, 644: 247
- 36 Wang J F, Gao S, Song P F et al. *Journal of Alloys and Compounds*[J], 2011, 509(34): 8567
- 37 Xu D K, Liu L, Xu Y B et al. *Materials Science and Engineering A*[J], 2006, 420(1-2): 322
- 38 Golmakaniyoon S, Mahmudi R. *Materials Science and Engineering A*[J], 2011, 528(15): 5228
- 39 Du Y Z, Qiao X G, Zheng M Y et al. *Materials Science and Engineering A*[J], 2015, 620: 164
- 40 Zhang L, Gong M, Peng L M. *Materials Science and Engineering A*[J], 2013, 565: 262
- 41 Guo F L, Yu H H, Wu C Y et al. *Scientific Reports*[J], 2017, 7(1): 8647
- 42 Kim W J, Hong S I, Kim Y S et al. *Acta Materialia*[J], 2003, 51(11): 3293
- 43 Agnew S, Yoo M, Tomé C. *Acta Materialia*[J], 2001, 49(20): 4277
- 44 Bohlen J, Yi S, Letzig D et al. *Materials Science and Engineering A*[J], 2010, 527(26): 7092
- 45 Stanford N, Sha G, Xia J H et al. *Scripta Materialia*[J], 2011, 65(10): 919
- 46 Stanford N, Barnett M R. *Materials Science and Engineering A*[J], 2008, 496(1-2): 399

Y 含量对 ZM21 镁合金组织和力学性能的影响

陈蓉¹, 胥钧耀¹, 张丁非¹, 余大亮², 冯靖凯¹

(1. 重庆大学 国家镁合金材料工程技术研究中心, 重庆 400044)

(2. 重庆科技学院, 重庆 401331)

摘要: 通过OM、SEM、EDS和XRD等研究了铸态及挤压态Mg-2Zn-1Mn-XY ($X=0, 0.8, 2.2$) (质量分数, 下同) 镁合金显微组织和力学性能。由实验结果可知, 稀土Y的添加, 不仅可以细化铸态及挤压态合金晶粒, 还可以弱化挤压态合金的基面织构强度, 从而同时提高合金的强度以及韧性。挤压态Mg-2Zn-1Mn-XY合金具有良好的力学性能, 与原始Mg-2Zn-1Mn合金相比, 屈服强度从164 MPa提高到204 MPa, 抗拉强度从237 MPa提高到298 MPa, 以及延伸率从12%增加到18%。

关键词: Mg-Zn-Mn 合金; 稀土 Y; 显微组织; 力学性能; 织构

作者简介: 陈蓉, 女, 1993年生, 硕士, 重庆大学材料科学与工程学院, 重庆 400044, 电话: 023-65112491, E-mail: chenrong00523@163.com